Carbohydrate Polymers 366 (2025) 123819

Contents lists available at ScienceDirect

Carbohydrate Polymers

journal homepage: www.elsevier.com/locate/carbpol

Sustainable aroma absorption: exploring the potentiality of a β-cyclodextrin and lactic acid supramolecular eutectic solvent☆

Emanuela Mangiacapre [a], Alessandro Triolo [b,*], Miriana Kfoury [c], Steven Ruellan [c], Fabrizio Lo Celso [d], Daniel J.M. Irving [e], Sophie Fourmentin [c,*], Olga Russina [a,b,**]

[a] Department of Chemistry, University of Rome Sapienza, Rome 00185, Italy
[b] Laboratorio Liquidi Ionici, Istituto Struttura della Materia, Consiglio Nazionale delle Ricerche (ISM-CNR), Rome 00133, Italy
[c] Univ. Littoral Cote d'Opale, UR 4492, UCEIV, Unite de Chimie Environnementale et Interactions sur le Vivant, 59140 Dunkerque, France
[d] Department of Physics and Chemistry, University of Palermo, Palermo, Italy
[e] Diamond Light Source Ltd., Didcot, Oxfordshire OX11 0QX, UK

ARTICLE INFO

Keywords:
Supramolecular
Hydrogen bonding
Low melting mixtures
Solvation
Task specific solvents
Sustainability

ABSTRACT

Supramolecular deep eutectic solvents (SUPRADESs), formed by combining cyclodextrins (CDs) with hydrogen bond donors, enhance solvation efficiency while retaining CD inclusion capabilities. This study presents the first detailed structural analysis of a SUPRADES composed of β-cyclodextrin (β-CD) and lactic acid (LA) (1:30 molar ratio) using Molecular Dynamics simulations and X-ray scattering. Results reveal a well-dispersed system where LA molecules form stabilising sheaths around isolated β-CDs, preventing coalescence through optimized hydrogen bonding and dispersive interactions. The SUPRADES significantly improved solubilisation and retention of water-insoluble trans-anethole (AN), demonstrating strong absorption capacity. While β-CD encapsulation of AN was limited, 2D ROESY NMR confirmed inclusion complex formation. These findings highlight the SUPRADES's unique microstructure and its potential as a sustainable, eco-friendly solvent for volatile organic compound (VOC) applications, offering insights for future green solvent design.

1. Introduction

Cyclodextrins (CDs) are natural cyclic oligosaccharides easily produced by the enzymatic degradation of starch and commonly contain six (α-CD), seven (β-CD), or eight (γ-CD) D-glucopyranose units linked by α-(1,4) glycosidic bonds. They exhibit a hollow truncated cone structure with varying cavity sizes, characterised by a relatively hydrophobic interior and a hydrophilic outer surface (El Achkar, Moufawad, et al., 2020). This unique architecture enables the formation of inclusion complexes with molecules that have low hydrophilicity and appropriate geometric sizes, driven by non-covalent host-guest interactions of a supramolecular nature (Crini et al., 2018a; Szejtli, 1998). Consequently, CDs find applications across diverse fields such as cosmetics, pharmaceutics, food, and catalysis to enhance the solubility or stability of guest compounds (Crini et al., 2018b; Ferreira et al., 2015; Gonzalez Pereira et al., 2021; Kfoury, Auezova, et al., 2015, 2019; Loftsson & Brewster, 1996; Marques, 2010). Although extensive research has focused on inclusion complexes in aqueous environments (Bhardwaj & Purohit, 2023; Connors, 1997; Kfoury et al., 2018; Kfoury, Auezova, et al., 2019; Kumar & Purohit, 2024; Rekharsky & Inoue, 1998; Saokham et al., 2018; Yu et al., 2015), few instances involve complex formation in water with the addition of a cosolvent (He et al., 2003; Kfoury, Geagea, et al., 2019; P. Li et al., 1999; Nakhle et al., 2020) or in organic solvents (Kida et al., 2011; Usacheva et al., 2020). Deep eutectic solvents (DESs), a new category of environmentally friendly solvents, can be considered as low-melting-temperature mixtures resulting from the combination of two or more different compounds, which exhibit interactions leading to enthalpic-driven negative deviations from thermodynamic ideality (Abranches & Coutinho, 2023; Martins et al., 2019). Typically, the structural organisation deriving from the components involves hydrogen bonding interactions; thus, the components are designated as hydrogen bond acceptor (HBA) and hydrogen bond donor (HBD) (Abbott et al., 2003; Smith et al., 2014). When two compounds capable of forming hydrogen bonds (HBs) are considered, the extended

☆ This article is part of a Special issue entitled: 'Cyclodextrin conference' published in Carbohydrate Polymers.

* Corresponding authors.
** Correspondence to: O. Russina, Department of Chemistry, University of Rome Sapienza, Rome 00185, Italy.
E-mail addresses: triolo@ism.cnr.it (A. Triolo), lamotte@univ-littoral.fr (S. Fourmentin), olga.russina@uniroma1.it (O. Russina).

https://doi.org/10.1016/j.carbpol.2025.123819
Received 30 January 2025; Received in revised form 18 April 2025; Accepted 26 May 2025
Available online 27 May 2025

hydrogen bond network formed is recognised as the primary factor contributing to the reduction of the melting point compared to an ideal mixture (Abranches & Coutinho, 2023; Martins et al., 2019; Smith et al., 2014). The advantage of DESs lies in their ability to serve as "designer-solvents": by carefully selecting their components, it is possible to adjust their properties, making them suitable for various applications (Abbott, 2022; Dwamena, 2019; Ünlü et al., 2019).

Leveraging the tunability of DESs, numerous studies are now exploring the potential synergies between CDs and DESs to develop new media with essentially unique properties. For instance, the addition of methyl-β-CD to a glycerol-based DES exhibited heightened efficacy in polyphenol extraction (Athanasiadis et al., 2018). Another study employing static headspace-gas chromatography (SH-GC) demonstrated an increase in volatile organic compounds (VOCs) solubilisation by incorporating CDs into DES, albeit with lower formation constants for complexes compared with those observed in water (Moufawad et al., 2019). Additionally, NMR studies have revealed complex formation within DESs for both nonsteroidal anti-inflammatory drugs (Dugoni et al., 2019) and VOCs (Di Pietro et al., 2019). More recently, researchers have explored the feasibility of crafting binary mixtures of CDs and other compounds to yield new media where DES's characteristic low melting point synergises with CDs' ability to encapsulate guest molecules. Notably, El Achkar et al. introduced a mixture of randomly methylated β-CD (RAMEB) and levulinic acid, which is devoid of a distinct melting/freezing point but exhibits significant prowess in solubilising *trans*-anethole (El Achkar, Moufawad, et al., 2020). Subsequent efforts involved a binary mixture comprising modified β-CD (specifically HP-β-CD) and levulinic acid, effectively entrapping and solubilising *trans*-anethole (El Achkar, Moura, et al., 2020). Considering levulinic acid's attitude as a hydrogen bond donor and/or acceptor in various DESs (Gutiérrez et al., 2022; G. Li et al., 2016; Maugeri & de María, 2012; Sánchez et al., 2019) and the ability of the aforementioned systems to maintain a low melting point alongside CDs' capacity to capture guest molecules through supramolecular interactions, these systems were coined as SUPRAmolecular DESs (SUPRADESs) (Janicka et al., 2022; Kfoury et al., 2022).

The development of SUPRADESs is only in its infancy, but recent years have witnessed a notable surge in interest in these media. For instance, a recent study showcased various SUPRADESs containing different CDs and lactic acid as effective media for headspace single-drop microextraction (HS-DME) coupled with high-performance liquid chromatography (Farooq et al., 2021). SUPRADESs have been used for the solubilisation of anti-inflammatory drugs (El Masri et al., 2022) and to capture volatile organic compounds (VOCs) of diverse nature (Gui et al., 2024; Kfoury et al., 2024). Understanding the interaction mechanisms among the various components of a SUPRADES and potential guest encapsulation is crucial. Triolo et al. provided a pioneering exploration into the structural organisation of the prototypical SUPRADES composed of heptakis(2,6-di-*O*-methyl)-β-cyclodextrin (DiMeβ-CD) and levulinic acid at a molar ratio of 1:27. Their findings revealed that the interplay between hydrogen-bonding and dispersive interactions prevents CD aggregation, maintaining a stable liquid phase and preserving the capability for inclusion complex formation (Triolo et al., 2023). A similar investigation was conducted on SUPRADES consisting of RAMEB and ethylene glycol at a molar ratio of 1:40, where the ability to solubilise $ChCl_3$ was attributed to the presence of van der Waals forces (Gui et al., 2024).

Recently, a supramolecular system composed of natural β-cyclodextrin (β-CD) and lactic acid (LA), in a 1:30 molar ratio, has been introduced and evaluated against a related system utilising maltodextrin. Therein, the β-CD-based SUPRADES demonstrated markedly superior retention capabilities for both (−)-limonene and (−)-terpinen-4-ol when compared to the maltodextrin-based system. This underscores the significant potential of cyclodextrins in maintaining encapsulation capacity when engaged in the SUPRADES environment. Moreover, the absence of a crystallization point for this SUPRADES has been assessed: only a glass transition at ca. -70 °C was detected, thus enabling the use of this solvent medium over a broad liquid window (Kfoury et al., 2024).

The proposed SUPRADES is fully environmentally sustainable as it is based on β-CD and LA, both of which are naturally occurring compounds (derived from potatoes, corn, maize, and cassava starches for β-CD and from corn, beets and cane sugar carbohydrates for lactic acid). Both SUPRADES ingredients are biodegradable, making the solvent eco-sustainable and more environmentally friendly compared to organic solvents, synthesized solvents (e.g., ionic liquid) and other DESs derived from less natural or synthetic chemicals.

We propose the hypothesis that β-CD and LA can effectively interact with one another, resulting in a stable and homogeneous solvent medium, as a consequence of an intricate balance of hydrogen bonding and dispersive interactions. However, this proposal can be disputable, especially considering the role played by β-CD hydroxyl groups in depressing β-CD solubility in protic solvents, such as water, glycerol or ethylene glycol. Taking into account the supramolecular nature of the solvent, we further hypothesise that this supramolecular medium will possess considerable absorption capacity for *trans*-anethole (AN), thereby affirming the significant role of β-CD's host capabilities. The validation of these hypotheses could signify a significant advancement: the effective retention of β-CD's inclusion capacity, while ensuring a substantial concentration of β-CD in the solvent medium, is a highly sought-after objective in supramolecular chemistry.

In this context, our study preliminarily aims at providing a detailed analysis on the structural architecture of the β-CD and LA (at 1:30 molar ratio) supramolecular medium, using Molecular Dynamics (MD) simulations supported by X-ray scattering experiments. We then explore the retention and absorption capabilities of this SUPRADES (with and without water additions) towards *trans*-anethole (AN). Ultimately, our goal is to develop and rationalise a system that remains in the liquid state even down to rather low temperature, preventing β-CD aggregation, and shows high absorption capacity for a VOC of significant interest.

2. Materials and methods

2.1. Materials

β-cyclodextrin (β-CD) was sourced from Wacker-Chemie (Lyon, France). L-Lactic acid (LA) (anhydrous, 98 %) was acquired from Fisher Scientific (France) and *trans*-anethole (AN) 99 % was provided by Aldrich (France). All compounds were utilised as received, and deionised water was employed in all procedures when necessary. The structures of the compounds used in this work are shown in Fig. 1.

2.2. Preparation of the β-CD:LA SUPRADES and its mixtures with water

The supramolecular DES (SUPRADES) β-CD:LA was obtained by heating and stirring technique. β-CD was combined with LA in a β-CD:LA molar ratio equivalent to 1:30. The mixture was heated at 333.15 K with constant stirring until a homogeneous liquid was achieved. The resulting SUPRADES remained in a liquid state at room temperature, with a water content of. 5.28 ± 0.22 % (Kfoury et al., 2024), determined using a Karl Fischer titration method with a DL31 Volumetric KF Titrator (Mettler Toledo DL31). SUPRADES-water mixtures were then prepared adding deionised water at different water contents (wt%). In particular, four different mixtures were produced with 10 wt%, 25 wt%, 50 wt%, and 75 wt% water.

For the investigation of AN retention, two additional mixtures were formulated: one comprising an aqueous solution of β-CD (at its maximum solubility in water, 18.5 mg/mL (Brewster & Loftsson, 2007)) and another containing LA and water, with amounts adjusted to match the molar ratio found in the pure SUPRADES between β-CD and LA.

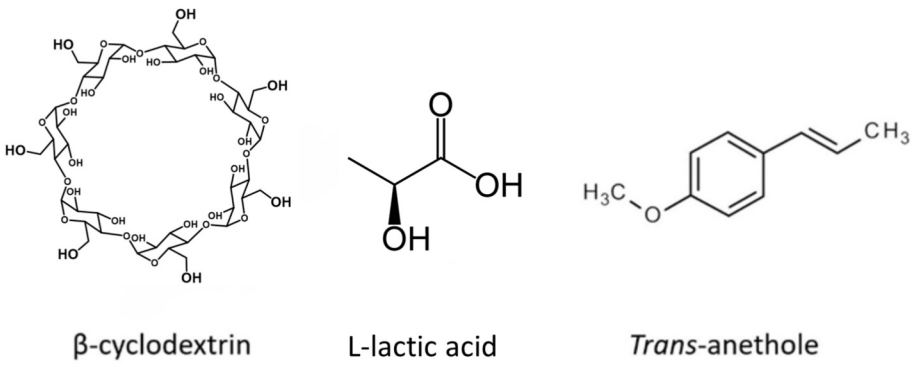

Fig. 1. Structure of the compounds used in this study.

2.3. X-ray scattering experiments

X-ray total scattering experiments were performed at the Diamond Light Source (UK), using the I15–1 XPDF beamline, with an energy of 76.69 keV (0.161669 Å). Data were acquired by a Perkin Elmer XRD 4343CT detector positioned 700 mm away, and for collecting low-angle scattering a beam stop was employed. The sample was inserted in a glue-sealed 1.5 mm borosilicate capillary and loaded onto the beamline via an automated robot system. The measurement, including relevant background and empty capillary data for processing, was taken over approximately 10 min and the sample was analysed at room temperature (Bracchini et al., 2024). The data were processed into 1D format using DAWN software. Corrections for background noise, absorption, polarisation, and Compton scattering were applied using GudrunX (Soper, 2011).

A Xeuss 2.0 Q-Xoom system (Xenocs SA, Sassenage, France) with a micro-focus Genix 3D X-ray source ($\lambda = 0.1542$ nm) and a two-dimensional Pilatus3 R 300 K detector that can be positioned at different distances from the sample was used to perform the Small Angle X-ray Scattering (SAXS) measurement at the SAXS Lab Sapienza. The measurement was conducted to cover a Q range of $0.04 < Q\ (Å^{-1}) < 3.5$ and data were collected at room temperature (ca. 293 K). The sample was inserted into a quartz capillary with a thickness of 1.0 mm and sealed with hot glue.

2.4. Computational details

Molecular dynamic calculations were performed through the GROMACS 2021.3 package (Hess et al., 2008; Van Der Spoel et al., 2005). Bonded and non-bonded parameters for the β-CD were derived from q4-MD force field (Cézard et al., 2011; Gebhardt et al., 2018; Zhang et al., 2012), while for the LA species an all-atoms potential OPLS-AA was used, obtained through the LigParGen webserver (Dodda, De Vaca, et al., 2017; Dodda, Vilseck, et al., 2017; Jorgensen et al., 1996; Jorgensen & Tirado-Rives, 2005).

The simulation was performed using a cubic box of 40 β-CD units and 1200 LA molecules, thus reproducing the experimentally used molar ratio 1:30; periodic boundary conditions were applied. Initial configurations were created by Packmol software (Martinez et al., 2009), the starting box dimension in both simulations was fixed at 6 nm. The equilibration phase was developed in many steps, starting with an NVT simulation at 400 K, followed by a series of NPT runs that gradually reduced the temperature to its final value of 350 K. Pressure was held constant for all systems at 1 bar, and a total of 12 ns equilibration runs were performed.

After the equilibration process, the system was run for 50 ns in a production run before generating a final 2 ns trajectory and saving it at a frequency of 1 ps for structural property calculation. Simulations were always evaluated against the energy and density profiles. We employed a velocity rescaling thermostat (Bussi et al., 2007) (with a time coupling constant of 0.1 ps) for the temperature coupling and a Parrinello–Rahman barostat (Parrinello & Rahman, 1981) (1 ps for the relaxation constant) while for the pressure coupling, during the production runs. The equations of motion were integrated using the Leap-Frog algorithm with a 1 fs time step. Cut-offs for the Lennard- Jones and real space part of the Coulombic interactions were set to 16 Å.

The Particle Mesh Ewald (PME) summation method (Darden et al., 1993; Essmann et al., 1995) was applied for the electrostatic interactions, with an interpolation order of 6 and 0.08 nm of FFT grid spacing. Structure factors and selected pair correlation functions and angular distribution functions were calculated through TRAVIS (Brehm et al., 2020; Brehm & Kirchner, 2011; Hollóczki et al., 2015). The gmx energy routine of Gromacs was used to evaluate the interaction energies between different moieties in the system, in terms of their dispersive (E_{disp}) and Coulombic (E_{Coul}) contributions.

2.5. Density and viscosity measurements

Density (ρ) and viscosity (η) measurements were conducted using a Stabinger SVM 3001 apparatus from Anton Paar. Temperature control was maintained within 0.005 °C. All measurements were performed under atmospheric pressure over the temperature range of 293.15–323.15 K.

2.6. Surface tension measurements

Surface tension (γ) was determined using the pendant drop method with the Attension-Theta Flex instrument (Biolin Scientific, Finland). The droplet of air is attached to an inverted needle immerged in the sample. Measurements were conducted at 293.15 K, and each sample was measured at least four times to ensure accuracy. The mean values and related errors were calculated and reported for each sample.

2.7. Static headspace-gas chromatography experiments (SH-GC)

The SH-GC experiments were performed utilising a Thermo Scientific™ TriPlus™ 500 Headspace Sampler connected to a TRACE™ 1300 Series GC featuring a flame ionisation detector and a DB624 column with nitrogen as the carrier gas. The GC column temperature stayed constant at 393.15 K throughout the experiments. Glass vials, with a volume of 22 mL, were prepared for headspace sampling, sealed, and kept at 303.15 K with stirring for 24 h to establish equilibrium between the liquid and gaseous phases. Subsequently, 1 mL of the gaseous phase was extracted from the vial and fed directly onto the chromatographic column for analysis (Kfoury et al., 2024).

2.7.1. Determination of vapour-liquid partition coefficients

The vapour-liquid partition coefficient (K) is a key parameter related to the mass distribution between the gas and liquid phases in equilibrium and it can be easily determined through the solute's solubility in the

liquid phase. It is calculated as the ratio of solute concentrations in the gas and liquid phases, using the following equation:

$$K = \frac{C_G}{C_L} \quad (1)$$

Here, C_G and C_L represent the concentrations of the solute in the gas and liquid phases, respectively. To determine the K values for the investigated mixtures, we employed a well-established procedure, which is a combination of two different methods, as already shown in previous studies (Gui et al., 2024, 2025; Villarim et al., 2022, 2024). We applied the phase ratio variation method described by Kolb and Ettre to determine the K values in water (Kolb & LS, 2006), while the vapour phase calibration method was employed to establish the VOC partition coefficients in the absorbent. A detailed description of the K values calculation can be found in previous works (Gui et al., 2024; Moura et al., 2017; Villarim et al., 2022, 2024). VOC was added at known concentrations to precise masses of the investigated mixtures (3 g) in vials with a 20 mL volume. After, samples were stirred under magnetic agitation and equilibrated for 24 h before SH-GC analysis at 303.15 K. The distribution of VOCs between phases occurred according to thermodynamically controlled equilibrium constants.

2.7.2. Determination of the formation constant with SH-GC

The calculation of the formation constant (K_f) for the β-CD/AN inclusion complex was calculated at 303.15 K using a titration technique established by Decock et al. (Decock et al., 2008). Vials were assembled by introducing a consistent amount of AN to 3 g of SUPRADES-water mixtures considering different β-CD concentrations (ranging between 0 and 0.34 M). Subsequently, the vials underwent treatment and analysis in accordance with the methodology outlined in the preceding section (Section 2.7) via SH-GC. Finally, an algorithmic method based on eq. (2) was applied to determine K_f value from the experimental data (Decock et al., 2008; Landy et al., 2000):

$$[\beta - CD/AN] = -\frac{1}{2}\sqrt{\left[\left(\frac{1}{K_f} + [\beta - CD]_T + [AN]_T\right)\right]} + \frac{1}{2}\left(\frac{1}{K_f} + [\beta - CD]_T + [AN]_T\right) \quad (2)$$

where [β-CD/AN] represents the concentration of the inclusion complex formed, while $[\beta\text{-CD}]_T$ and $[AN]_T$ denote the initial concentrations of β-CD and the volatile guest, respectively.

2.7.3. Retention study

Vials were prepared by adding an appropriate quantity of AN to previously measured 3 g of SUPRADES-water mixtures (0,10, 25, 50, 75, and 100 wt% water). The percentage of retention was determined using the following formula:

$$\text{Retention}\ (\%) = \left(1 - \frac{A_m}{A_w}\right) \times 100 \quad (3)$$

Here, A_m and A_w represent the peak areas of AN in the SUPRADES-water mixtures and pure water, respectively.

2.8. NMR study

A Bruker Avance III spectrometer with a multinuclear z-gradient BBFO probe head and a 400 MHz operating frequency for the proton nucleus was used for the NMR experiment. Standard 5-mm NMR tubes with D2O inserts were utilised, and the probe temperature was set at 30 °C. Using the troesyph off-resonance pulse program (from the Bruker library), a mixing time of 800 ms was applied during spin-lock for the 2D-ROESY spectrum of the β-CD/AN complex in the β-CD:LA mixture. 512 tests with 142 scans in F1 and a temporal domain of 2048 K in F2 were used to implement the States-TPPI approach. The sample was prepared as follows: approximately 300 mg of β-CD and 700 mg of LA were used for SUPRADES preparation, followed by the addition of 250 μL of D_2O and 5 μL of pure AN. The mixture was filtered before performing the NMR measurements.

3. Results and discussion

3.1. β-CD:LA structural features

The liquid structure organisation of the β-CD:LA SUPRADES was characterised by means of wide-angle X-ray Scattering (WAXS) and small-angle X-ray Scattering (SAXS). When comparing the experimental and simulated WAXS patterns, particularly in the Q-range > 2 Å^{-1}, we observe a generally good agreement. Despite deviations in intensity at Q values <2 Å^{-1} (likely due to the finite size of the simulation box), the overall similarity confirms the success of MD calculations in reproducing structural features.

The experimental SAXS pattern (inset of Fig. 2) differs from the one of related systems, such as the β-CD-Reline mixture (Triolo et al., 2020), β-CD in the [C2mim][OAc] ionic liquid (Triolo et al., 2022), and finally the aqueous solution of β-CD (Kusmin et al., 2008), due to the high β-CD concentration in the present SUPRADES, as compared to the other more dilute mixtures. On the other hand, the present experimental pattern is comparable to that reported for the other SUPRADES DiMeβ-CD-LevAc, where comparable CD content was considered (Triolo et al., 2023), consistently with the observation that no CD flocculation occurs, and the latter are distributed homogeneously in the sample. This observation is further supported by the MD simulation snapshot in Fig. 3, where one can observe that β-CDs maintain close to each other (that is reasonable, considering the CD content), but without forming fully segregated aggregates.

To further investigate the structural organisation of the SUPRADES, we then explored the outcome of the MD simulation trajectory. Specifically, we examined intermolecular interactions among SUPRADES components by studying various Radial Distribution Functions (RDFs) or g(*r*)s.

Fig. 4 presents selected g(r) functions highlighting specific correlations between the β-CD centre of mass (#2) and either the #2 position of lactic acid (LA), or other LA sites (namely O1 and C3). To distinguish correlations occurring inside versus outside the β-CD walls, we also determined the RDF between the centre of mass of β-CD (#2β-CD) and all other β-CD atoms within the macromolecule (Triolo et al., 2023),

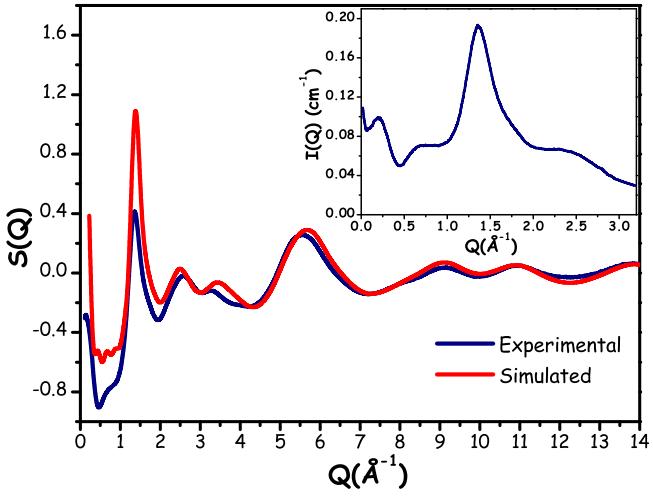

Fig. 2. Experimental (blue line) and computed (red line) X-ray weighted normalised structure factors (S(Q)) for the β-CD:LA SUPRADES system at room temperature. In the inset, the experimental SAXS data for the probed system at room temperature are shown.

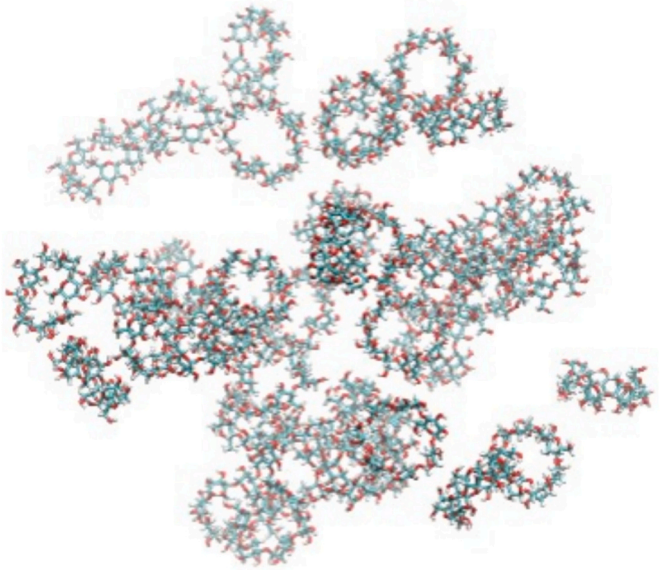

Fig. 3. Representative snapshot of the studied β-CD:LA SUPRADES, where only the β-CD molecules are shown (licorice representation).

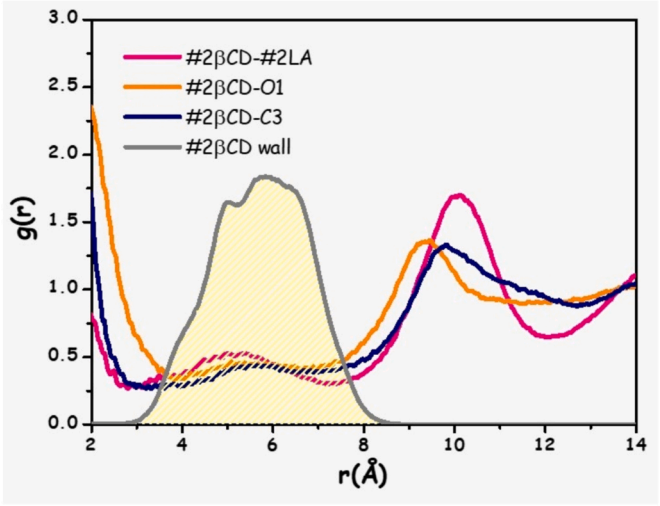

Fig. 4. Selected MD-computed Radial Distribution Functions (RDFs) between β-CD centre of mass (indicated as #2β-CD) and LA centre of mass (indicated as #2LA) and other relevant atoms. The yellow shadowed area is related to the intramolecular RDF between #2β-CD and all other β-CD atoms.

represented by the yellow pattern in Fig. 4. Accordingly, at distances $r <$ 3 Å, we monitor the content of the CD cavity, while for $r >$ 8 Å, we probe the external environment surrounding the reference CD.

The #2β-CD-#2LA g(r) shows a distinct peak closer to the CD wall, centred at about 10 Å, suggesting that CD solvation in the SUPRADES is sustained by LA molecules that are very close to the CD wall.

Similarly to the DIMEB:LevA system, by integrating the #2β-CD-#2LA g(r) up to 3 Å, one detects ca. 1 LA molecule enclosed inside the β-CD (Triolo et al., 2023). There is limited LA presence within a distance range between 3 Å and 8 Å. Then, by integrating up to 12 Å (i.e. up to first solvation shell), one finds that ca. 35 LA molecules are located, on average, around the reference β-CD; such a quantity closely matches the chosen molar ratio between β-CD and LA, which was chosen to achieve a stable mixture. This observation confirms the importance of selecting an optimal molar ratio between CD and molecular compound to ensure an effective CD solvation in SUPRADES (Triolo et al., 2023).

Based on these observations, the structural organisation of the SUPRADES system appears to be characterised by surrounding layer of LA molecules that effectively keeps the cyclodextrins well-separated and, hence, avoids the β-CD coalescence that is observed, e.g. in water.

A more thorough examination of the RDFs depicted in Fig. 4 provided additional insights into the LA organisation surrounding β-CD. The LA oxygen atoms (data shown for O1 only) distribute around the β-CD wall, as indicated by a well-defined, sharp peak centred around 9 Å for the #2β-CD-O1 correlation.

Furthermore, in contrast to the DiMeβ-CD:LevAc SUPRADES system, where no distinct correlations were observed, the interaction between β-CD and the methyl carbon (C3) of LA exhibits a relatively intense and well-structured feature, centred around approximately 10 Å (Triolo et al., 2023). This difference might be related to the different size between LA and the levulinic acid and represents a hint on how neighbour β-CD molecules are maintained separated to ensure their homogeneous distribution in the system.

Considering that β-CD presents 21 HB donor sites and 35 HB acceptor sites, while LA includes three acceptor oxygens (O1, O2, and O3) and two hydrogens (H2 and H3) that can serve as HB donors, we interrogated our MD trajectory for the conceivable hydrogen bonding interactions. Most likely, these will be the predominant interactions taking place in this system.

The hydrogen bonding interactions within the examined system were primarily analysed through the computation of RDFs involving the possible correlations between the β-CD hydrogen bond acceptor/donor sites and the LA hydrogen bond acceptor/donor moieties.

In **Fig. S1** a) to c) of the **ESI**, we monitored the correlations involving the hydroxyl hydrogens of β-CD (Ha and Hd, belonging to the upper and lower rims, respectively, see Scheme 1), which serve as donors to the LA oxygen atoms (O1, O2 and O3). Except for the correlations involving the O1 oxygen, where the feature around 2 Å appears as a shoulder to a primary peak at approximately 3.5 Å, we clearly observe well-defined peaks centred around 2.0 Å. These peaks are indicative of the establishment of hydrogen bonding interactions between lactic acid and β-CD.

A clear preference emerges for the LA oxygen atoms to interact with the Ha hydroxyl group. This is evidenced by g(*r*)s displaying the highest intensity and the largest number of nearest neighbours compared to those involving Hd (Table 1).

The preference for Ha is attributed to the greater mobility and accessibility of this hydroxyl hydrogen compared to Hd. Moreover, one should also consider the increased freedom resulting from Ha lower propensity to engage in intramolecular hydrogen bonding, at odd with Hd sites, which have neighbour hydroxyl groups in adjacent glucopyranose rings.

Furthermore, it is evident that the examined hydroxyl hydrogens of β-CD predominantly engage in hydrogen bonding interactions with the carboxylic oxygen (O3) of LA.

The investigation into hydrogen bonding interactions within the studied system was extended with the aid of **Fig. S2** in the **ESI**, illustrating correlations between all the acceptor sites of β-CD (Oa-Od sites in Scheme 1) and H2 and H3 in LA. In **Fig. S2 (a)**, the g(r)'s Oa-H2 and Od-H2 are characterised by intense and well-defined peaks at 1.8 Å. In this case, it emerges again the enhanced tendency of β-CD primary hydroxyl groups to engage into HB interactions: specifically, when integrating over a distance of about 2.5 Å, we observe a value of approximately 0.40 for the Oa-H2 correlation and around 0.21 for the Od-H2 correlation, suggesting H2 preference to interact with Oa rather than Od. On the other hand, Oa-H3 and Od-H3 g(r)s show only weak peaks at ca. 2 Å, suggesting that Oa and Od prefer engaging hydrogen bonding interactions with H2 rather than H3 sites in LA, likely due to the more acidic nature of a carboxylic hydrogen compared to that of a hydroxyl hydrogen.

Concerning the other β-CD oxygen atoms (Ob and Oc), their engagement into correlations with either H2 or H3 in LA are

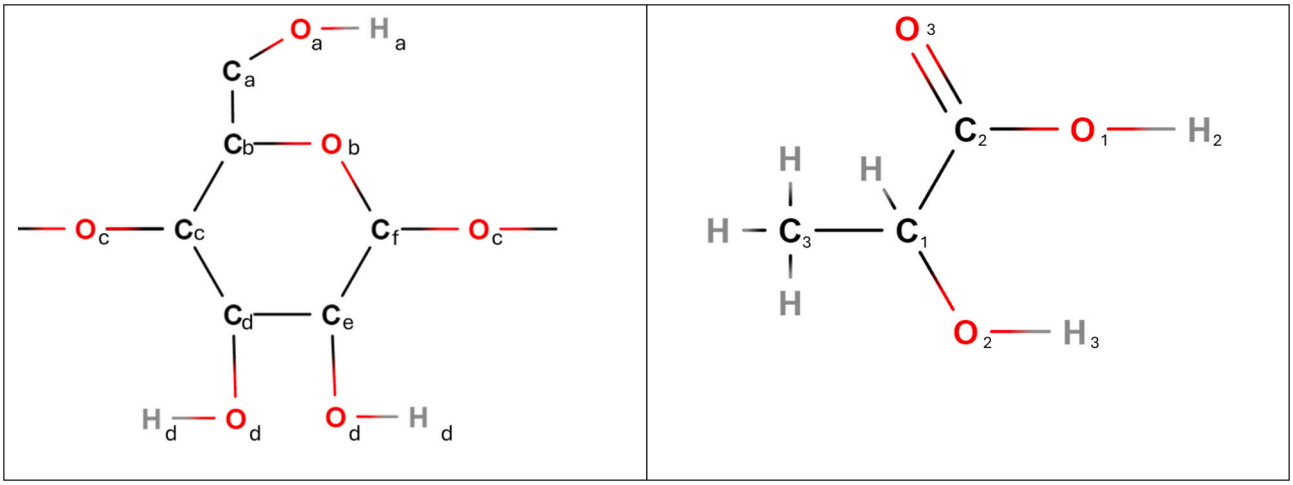

Scheme 1. Schematic representation of a β-CD monomer (left, indicated as CD in the MD investigation) and LA (right).

Table 1
Number of nearest oxygen neighbours N(r) related to the hydrogen bonding correlations between the hydroxyl hydrogens of β-CD (Ha and Hd) and the oxygen atoms of LA (O1, O2 and O3).

Correlation	Solvation shell extent (Å)	N(r)
Ha-O1	3.0	0.22
Hd-O1	3.0	0.16
Ha-O2	3.0	0.29
Hd-O2	3.0	0.20
Ha-O3	3.0	0.37
Hd-O3	3.0	0.31

characterised by much weaker g(r) peaks, indicating weaker hydrogen bonding correlations (**Fig. S2** (b)).

The system exhibits a highly intricate hydrogen-bonding network, further modulated by the presence of intramolecular hydrogen bonds between adjacent cyclodextrin units. As shown in **Fig. S3**, the secondary hydroxyls of β-CD participate in strong intramolecular hydrogen bonding interactions. The combined distribution function (CDF) for a representative correlation between the Hd hydrogen of one glucopyranose unit and the Od oxygen of an adjacent glucopyranose unit reveals a distinct hot spot. This hot spot is centred at a distance of approximately 1.8 Å with an angular range of 0–30°, consistent with strong hydrogen bonding interactions.

Hydrogen bonding interactions between LA molecules were also evaluated. **Fig. S4** in the **ESI** displays the correlations involving both the carboxylic and hydroxyl groups of LA. Once again, the carboxylic region demonstrates a strong propensity to engage into strong hydrogen bonds. Specifically, very sharp and intense peaks are observed around 1.8 Å for the O3-H2 correlation, which also shows the highest number of nearest neighbours (approximately 0.5 at 3.0 Å). Additionally, a distinct tendency for the hydroxyl group, consisting of O2 and H3, to establish correlations with the carboxylic moiety of another LA molecules is evident. This is reflected in the clear presence of sharp and intense peaks around 2.0 Å for both O2-H2 and O3-H3 correlations.

We next explored the existence of correlations between LA molecules and β-CD which are not driven by HB interactions. β-CD oxygen atoms and LA carbon atoms g(r)s are shown in **Fig. S5** in the **ESI**: while interactions involving Ob and Oc with all LA carbon atoms exhibit relatively unstructured peaks, distinct patterns emerge for the cases of Oa and Od, likely due to molecular ordering driven by HB interactions.

Correlations between selected carbon atoms of cyclodextrin (specifically, those near the ether groups and the carbon directly bonded to the hydroxyl group) and LA methyl carbon atoms are shown in **Fig. S6** in the **ESI**. Relatively defined peaks are observed, though all have intensities maintain below unity. The most prominent and structured feature, corresponding to the Ca—C3 correlation, with a peak centred around 4.0 Å, is driven by HB interactions.

Structured features are also evident for the carbon atoms near the ether oxygens of cyclodextrin, specifically Cc and Cf, highlighting the existence of weak hydrophobic interactions between apolar portions of the SUPRADES. Such an interaction, though of weak extent, turns out to be fundamental to avoiding adjacent β-CD to coalesce and phase separate, as it happens with β-CD dissolved in water.

The above described intricacy between hydrogen bonding and dispersive interactions leading to a structurally homogeneous SUPRADES is reflected by the interaction energy between β-CD and LA. We decomposed the interaction energy between these moieties into dispersive (van der Waals interactions, E_{disp}) and coulombic (E_{Coul}, including hydrogen bonding) contributions and obtained $E_{disp} = -16{,}800$ kJ/mol and $E_{Coul} = -14{,}650$ kJ/mol for the two terms. Their very similar values reflect the strong interplay between these two kinds of interactions in SUPRADES, analogously to what was detected for other SUPRADES systems (Triolo et al., 2023).

Overall, the structural organisation of the system manifests as remarkably complex; it is primarily driven by the strong, diverse hydrogen bonding interactions between β-cyclodextrin (β-CD) and lactic acid (LA), but with a fundamental role played by dispersive interactions. An extensive solvation network is generated as a result, which effectively ensures the separation of β-cyclodextrin molecules, thus maintaining the mixture as overall homogeneous.

The emerging solvation scenario is expressed by a sort of LA sheath wrapping around β-CD walls, where LA molecules prevalently interact with β-CD through hydrogen bonding interactions, with the establishment of weak dispersive interactions between apolar moieties.

In this scenario, the stoichiometric ratio between β-CD and LA most likely plays a crucial role in shaping and stabilising the structural organisation, by promoting a balance between polar and dispersive interactions, thus effectively maintaining cyclodextrins separated between each other and preventing aggregation.

3.2. SUPRADES-water mixtures characterisation

The experimental density and dynamic viscosity values for the different SUPRADES-water mixtures are reported as a function of the % wt. water content, in **Tables S1** and **S2**, respectively, in the **ESI**. Both density and dynamic viscosity values are shown as a function of temperature in the temperature range 293.15–323.15 K. The temperature dependence of the reported parameters (Fig. 5) was described with two different equations: a quadratic relationship for the density and the

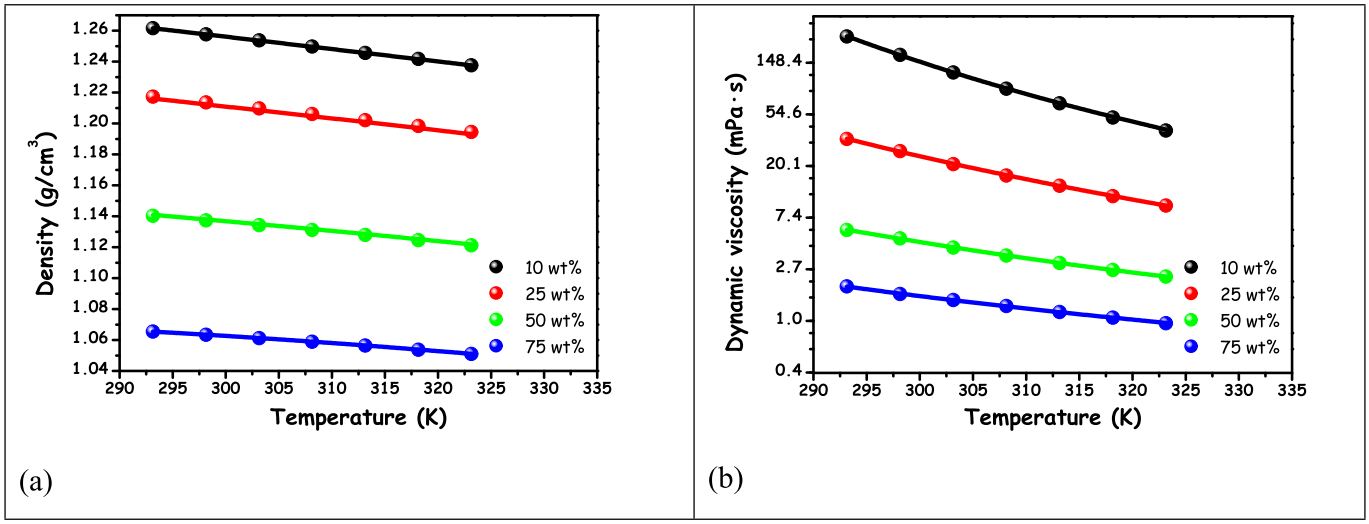

Fig. 5. Experimental values for the denisty (a) and the dynamic viscosity (b) of the SUPRADES-water mixtures. Solid lines represent the fits for both parameters.

Vogel-Fulcher-Tamann model for the dynamic viscosity. The corresponding fitting parameters are listed in **Table S3** in the **ESI**. Since the dynamic viscosity of the pure SUPRADES at 303.15 K does not vary with the shear rate, it can be defined as a Newtonian fluid, specifically showing a dynamic viscosity of 1.82 ± 0.19 Pa•s (Kfoury et al., 2024). It is important to highlight that the higher viscosity compared with traditional DESs or LTTMs is possibly attributed to the robust hydrogen bonding network characteristic of these supramolecular mixtures (Triolo et al., 2023).

Given this high value for dry SUPRADES, we were able to measure the density and dynamic viscosity only for the SUPRADES-water mixtures.

Although our experimental investigation did not specifically investigate dry SUPRADES, it is worth comparing with findings from other pure supramolecular mixtures. Chengmin et al. highlighted a decrease in these parameters with increasing temperature for different RAMEB and CRYSMEB-based SUPRADESs, suggesting that, in the framework of VOCs absorption, higher absorption temperatures enhance fluidity (Gui et al., 2024, 2025). A similar trend has been noted for various SUPRADESs based on levulinic acid and modified β-CD (El Achkar, Moura, et al., 2020).

The specific effect of water content on density and dynamic viscosity was investigated at 298.15 K and it is presented in Fig. 6. The dependence on water exhibits two distinct trends for the two physical variables under investigation: density shows a clear linear decrease, whereas dynamic viscosity follows an exponential decay.

In line with RAMEB-based supramolecular systems, there is a decrease in dynamic viscosity with increasing water content, leading to enhanced fluidity (El Masri et al., 2022). A similar trend is evident in various low melting mixtures incorporating β-CD derivatives and *N,N′*-dimethylurea, although the observed patterns lack systematicity compared with our findings (Jérôme et al., 2014) (Fig. 6, (b)).

This result highlights the potential to modulate key properties such as fluidity, which is crucial for practical applications. As shown in Fig. 6, dynamic viscosity significantly decreases from 10 wt% to 25 wt% water content while maintaining good absorption capacity for AN (as further discussed in the next section). This decrease may be attributed to the interference of water with the strong hydrogen bond network formed by β-CD and LA, making it more flexible, as previously observed in various DESs (Kivelä et al., 2022; López-Salas et al., 2019; Shah & Mjalli, 2014).

Next, the impact of water on the surface tension (γ, mN/m) of SUPRADES-water mixtures was examined at 293.15 K. The corresponding data are shown in Fig. 7.

Surface tension raises with increasing water content, following an exponential trend described by eq. 3 in the **ESI**. Currently, there are no existing studies on the surface tension of SUPRADESs. However, we can compare our results with those obtained for traditional LA-based DESs, which exhibit a different behaviour. For example, for the case of ChCl:LA (1:2) DES, surface tension remains nearly constant with increasing water content at 293.15 K, observing an increase only at a water molar fraction

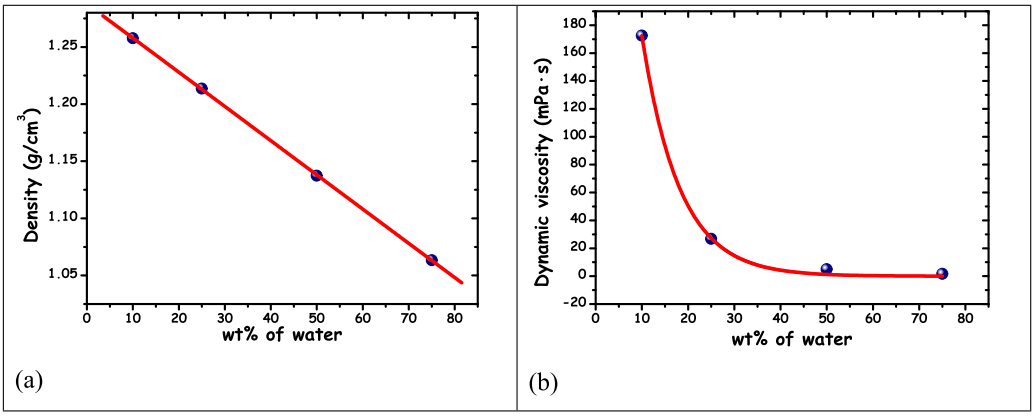

Fig. 6. Relationship between density and water content (wt%) at 298.15 K (a). Relationship between dynamic viscosity and water content (wt%) at 298.15 K (b). The solid red lines represent the data interpolation.

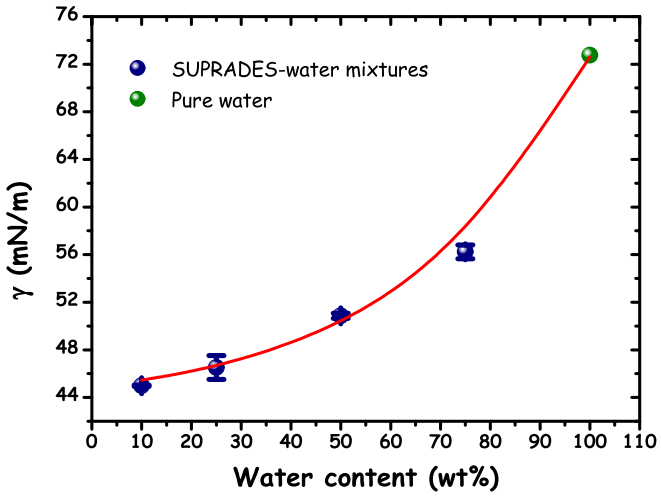

Fig. 7. Surface tension as a function of water content (wt%) at 293.15 K. The red solid line is related to the employed fitting procedure. The green dot represents the surface tension value of pure water (Vargaftik et al., 1983).

$x_{H2O} > 0.9$ (Chen et al., 2019). Conversely, Savi et al. observed a reduction in surface tension at 298 K for the LA:glucose (5:1) NADES as water content increased to achieve a final molar ratio of 5:1:3 (LA: glucose:water) (Savi et al., 2019). Similarly, in a NADES composed of betaine (BET) and LA in a molar ratio of BET:LA 1:2, a decrease in surface tension is noted with higher water content (Mohd Fuad & Mohd Nadzir, 2022).

The decrease in surface tension with lower water content (Fig. 7) can be attributed to the distinct composition of our SUPRADES compared to LA-based DESs. Its complex hydrogen bond network (discussed in the MD section) may disrupt water's intermolecular interactions, reducing surface tension. The same behaviour was observed in aqueous solutions of HP-β-CD (hydroxypropyl-β-CD): as its concentration in aqueous solutions increases, a noticeable decrease in surface tension is observed (Häusler & Muller-Goymann, 1993; Motoyama et al., 2009). This effect was attributed to the strong hydrogen bonding interactions between HP-β-CD and water molecules(Khuntawee et al., 2017), which may easily disrupt the HB network of water. As a result, increasing HP-β-CD concentrations lead to a reduction in surface tension.

Additionally, it is important to consider that pure SUPRADES has a lower surface tension than water (approximately 44.97 mN/m from the trend shown in Fig. 7), thus the SUPRADES/water mixture gradually approaches water's surface tension as the system shifts from water-in-DES to DES-in-water.

3.3. Trans-anethole absorption

AN is a prominent constituent of star anise and is renowned for its natural flavouring properties and antimicrobial attributes, which enhance food preservation. Despite its benefits, AN's utility is hampered by its high volatility and minimal solubility in water, along with susceptibility to degradation from air, light, or heat during food processing. To overcome these limitations, inclusion complexes with CDs offer a promising solution (Kfoury, Auezova, et al., 2014; Kfoury, Landy, et al., 2014). Therefore, the capacity of the investigated SUPRADES to absorb/retain AN was evaluated using SH-GC. In particular, the absorption was first evaluated by calculating the partition coefficients (K) of AN in pure SUPRADES and in the various SUPRADES-water mixtures at 303.15 K. The obtained values are presented in Table 2, along with the ratios $K_{water}/K_{absorbent}$. All experiments were conducted at the same equilibrium time, allowing for direct comparison of the obtained K values with those in water.

First, it is evident that the AN absorption in the investigated SUPRADES-water mixtures decreases with higher water content (wt%). This trend is reflected in the rising K values, indicating reduced VOC absorption. Particularly noteworthy is the exceptional retention efficiency of pure SUPRADES, which exhibits up to a 300-fold higher absorption efficacy for AN than pure water, as indicated by the partition coefficients. Equally remarkable is the value observed in the LA-water mixture and the absorption capability demonstrated by β-CD in water (refer to Table 2).

Table 2
Partition coefficient (K) values of *trans*-anethole (AN) in water and in the tested absorbents and ratios $K_{water}/K_{absorbents}$ at 303.15 K. [(a)]this work and [(b)] El Achkar et al.(El Achkar, Moura, et al., 2020).

Absorbent	K	$K_{water}/K_{absorbent}$
Pure SUPRADES	$8.88 \bullet 10^{-5}$	306
SUPRADES with 10 wt% water	$1.69 \bullet 10^{-4}$	161
SUPRADES with 25 wt% water	$1.81 \bullet 10^{-4}$	150
SUPRADES with 50 wt% water	$1.23 \bullet 10^{-3}$	22
SUPRADES with 75 wt% water	$1.96 \bullet 10^{-3}$	14
β-CD with 98 wt% water	$2.23 \bullet 10^{-3}$	12
LA with 30 wt% water	$2.99 \bullet 10^{-4}$	91
Pure water	$2.72 \bullet 10^{-2(a)}$ $1.29 \bullet 10^{-2(b)}$	1

Water influence can be attributed to the transition, at low water content, from a water-in-DES system to a DES-in-water one. This shift progressively reduces the AN solubility (due to its poor solubility in pure water), leading to a decrease in the partition coefficient.

AN absorption has been previously assessed in other supramolecular mixtures comprising levulinic acid (utilised as HBD) and various modified β-CDs (acting as HBAs). Of significant note is the outstanding efficacy displayed by the β-CD:LA SUPRADES, yielding a K value comparable to those obtained in the HPBCD:Lev, CRYSMEB:Lev, and Captisol®:Lev mixtures (El Achkar, Moura, et al., 2020). Through SH-GC measurements, the solubility of AN was assessed in a RAMEB-based supramolecular DES, revealing a 1300-fold increase in solubility compared with that observed in pure water (El Achkar, Moufawad, et al., 2020).

3.4. Determination of the formation constant

To investigate the ability of β-CD to encapsulate and dissolve AN, the formation constant of the β-CD/AN inclusion complex was determined at 303.15 K using SUPRADES-water mixtures (details concerning the

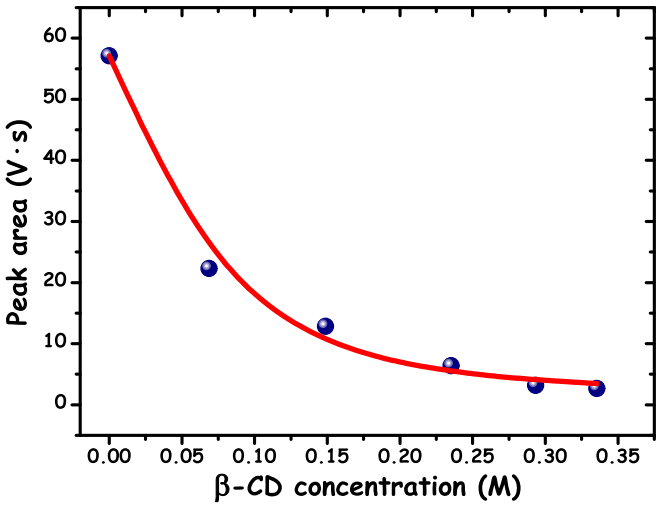

Fig. 8. Representation of the experimental peak area values obtained from the SUPRADES-water mixtures (blue spheres) compared with the theoretical titration curve (the red line) for a 1:1 complex.

samples are in Table S6 of the ESI). The formation constant value (K_f) of the β-CD/AN complex, equal to 57 M^{-1}, was determined through algorithmic treatment aimed at minimising the difference between the experimental and theoretical peak area values. Fig. 8 displays both the experimental peak area values and their theoretically derived counterparts.

The observed variations in the peak area values for the tested mixtures closely align with a 1:1 host/guest complex, as evident from Fig. 8. It is apparent that the experimental data points align well with the theoretical curve. Although the obtained complex formation constant (K_f) may appear relatively low compared with the value of 1040 M^{-1} obtained in water (Kfoury, Auezova, et al., 2014), the use of such SUPRADES can enhance both AN solubility and absorption. It is worth noting that while other systems employing β-CD do not yield favourable results for the solubility and/or absorption of AN, they exhibit higher K_f values. For instance, a study utilising NMR experiments assessed the K_f of the β-CD/AN complex at 1040 M^{-1}, despite demonstrating low solubility of AN, which is not directly correlated with the high K_f value obtained (Donze & Coleman, 1993). Similar observations can be made for other investigations employing SH-GC or UV–vis techniques. One study documented a K_f of 542 M^{-1} using UV–vis and 497 M^{-1} with SH-GC, both conducted on various aqueous β-CD solutions. In addition, a K_f of 441 M^{-1} was obtained when phosphate buffer (PBS) was added to the solutions (Kfoury, Auezova, et al., 2014). Other UV–vis assessments on β-CD solutions yielded a K_f of 542 M^{-1} (Kfoury, Landy, et al., 2014), whereas SH-GC experiments yielded a K_f of 630 M^{-1} (Ciobanu et al., 2013). Despite the higher K_f values observed in the aforementioned studies, less effective retention and solvation capabilities were achieved.

The decrease in K_f value could be attributed to the fact that at high SUPRADES wt% content, AN experiments more favorable interactions with the surrounding solvent molecules, which in turn disfavor the complex formation with β-CD. This induces a decrease in the solvatophobic forces, the governing forces for the inclusion complex (Nakhle et al., 2024).

3.5. Retention study using SH-GC

The capacity of the studied SUPRADES to retain AN was assessed using SH-GC as a function of water content. The findings are illustrated in **Fig. S7** in the **ESI**.

Initially, we can note an increase in the retention capacity for AN as the water content (wt%) decreases. Interestingly, this retention ability, along with AN absorption, remains notably high even when the investigated SUPRADES is mixed with water, as previously demonstrated by the calculation of partition coefficients (k) (refer to **section 3.3**).

Furthermore, it is noteworthy that the plot depicted in **Fig. S7** exhibits a trend that refers to the usual titration curve observed for 1:1 CD inclusion complexes. This observation aligns with other β-CD based systems (Kfoury, Balan, et al., 2015; Kfoury, Landy, & Fourmentin, 2019), particularly with the β-CD:LA SUPRADES, for which the evaluation of (−)-limonene and (−)-terpienen-4-ol has already been conducted (Kfoury et al., 2024). Similar trends were observed in various aqueous solutions of ChCl:Urea 1:2 DES (Reline) (Nakhle et al., 2023).

3.6. NMR study

As previously indicated by SH-GC and UV–vis analyses, the β-CD within the investigated SUPRADES can indeed establish inclusion complexes with the anethole. However, given that β-CD functions as a constituent of the solvent in this scenario, rather than as a solute, the sole method to confirm complex formation is 2D ROESY NMR spectroscopy. Fig. 9 presents a section of the contour plot from the ROESY spectrum of AN within the examined SUPRADES.

From Fig. 9, it is evident that there is a notable correlation between the H1 and H2 protons of AN and the inner proton of β-CD indicating that the phenyl ring of AN is indeed included in the β-CD cavity. This finding conclusively demonstrates that β-CD, despite being a solvent component rather than a solute, still possesses the capability to form inclusion complexes with guest molecules.

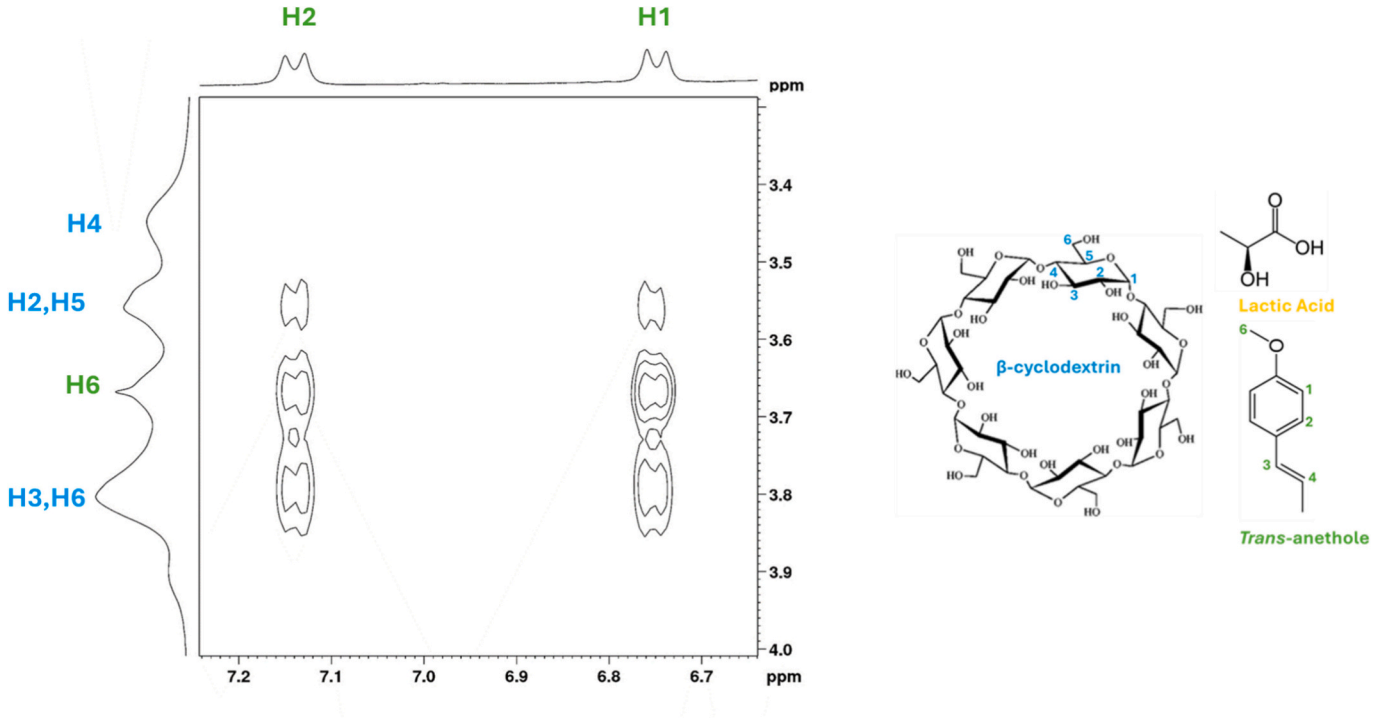

Fig. 9. ROESY spectrum of β-CD/AN complex in the β-CD:LA SUPRADES (spectra recorded with a D_2O insert).

4. Conclusions

This study provides, for the first time, a comprehensive description of the structural architecture of a β-CD and LA-based SUPRADES, highlighting its promising a) stability against phase separation and b) complexing capability towards drugs and aromas. Our investigation into the structural organisation of the pure SUPRADES, combining MD simulations and S-WAXS experiments, reveals a complex architecture which is characterised by a homogeneous β-CD distribution in the matrix and by the notable absence of β-CD aggregation. The study reveals that β-CD are surrounded, on average by ca 35 LA molecules, thus reflecting the ideal stoichiometric ratio that was formulated to obtain the stable SUPRADES. Moreover, the crucial role of LA-β-CD intermolecular hydrogen bonding in maintaining an efficient cyclodextrin solvation is assessed, with the observation of a multiform hydrogen bonding network, involving β-CD hydroxyl groups and LA carboxyl group. More importantly, we assess the fundamental co-presence of weak dispersive interactions between LA and β-CD apolar moieties, integrating the HB-driven solvation and prevailing on inter-CD hydrophobic coalescence. This solvation scenario involves the formation of a LA sheath surrounding isolated β-CD: in this respect, the ideal LA-β-CD stoichiometric ratio plays a key role in shaping and stabilizing this complex arrangement, facilitating a balance between polar and dispersive interactions. These results support our hypothesis of a complex interplay between HB and dispersive interactions maintaining the SUPRADES formulation stable and homogeneous.

A systematic evaluation of the SUPRADES absorption and retention capability towards AN, using vapour-liquid experiments and NMR investigations, was also carried out. SH-GC experiments demonstrate the impressive absorption capability of SUPRADES, even with minimal water content (specifically, 10 wt% and 25 wt%), as evidenced by significantly lower partition coefficients (k) compared to pure water. Determination of the complex formation constant (K_f) through titration methods highlights the limited encapsulation ability of β-CD, despite its solubility and retention capabilities. 2D ROESY NMR experiments confirm the formation of a β-CD/AN inclusion complex, indicating strong correlations between the β-CD cavity protons and the AN phenyl protons. We then provide support to the initial hypothesis on the preservation of β-CD's inclusion capacity at the elevated concentration achieved in the SUPRADES formulation.

Overall, this study provides a description and rationalisation for structure and host-guest functionality of a supramolecular eutectic medium, paving the way for the formulation of novel types of sustainable media for aromas, drugs, VOCs etc. encapsulation.

CRediT authorship contribution statement

Emanuela Mangiacapre: Investigation, Formal analysis, Data curation. **Alessandro Triolo:** Writing – review & editing, Writing – original draft, Supervision, Project administration, Investigation, Funding acquisition, Conceptualization. **Miriana Kfoury:** Validation, Supervision, Methodology, Investigation, Formal analysis. **Steven Ruellan:** Supervision, Investigation, Formal analysis, Data curation. **Fabrizio Lo Celso:** Software, Investigation, Formal analysis, Data curation. **Daniel J.M. Irving:** Investigation. **Sophie Fourmentin:** Writing – review & editing, Validation, Supervision, Resources, Project administration, Methodology, Data curation, Conceptualization. **Olga Russina:** Writing – review & editing, Writing – original draft, Supervision, Project administration, Investigation, Funding acquisition, Data curation.

Declaration of competing interest

The authors declare that they have no known competing financial interests or personal relationships that could have appeared to influence the work reported in this paper.

Acknowledgments

This work has been partially supported by the University of Rome Sapienza Project: “Supra-DES in action” (AR123188A08DF1D1). Expert support from Dr. A. Del Giudice and access to the SAXS-Lab at the University of Rome Sapienza is acknowledged.

Research at ISM-CNR was partially supported by the project ECS00000024 “Ecosistemi dell'Innovazione”— Rome Technopole of the Italian Ministry of University and Research, public call n. 3277, PNRR—Mission 4, Component 2, Investment 1.5, financed by the European Union, Next Generation EU.

This work was also partially supported by PRIN2022 (“SEED4-GREEN”), sponsored by the European Union, Next Generation EU, Missione 4 Componente 1 (RG11715C7CC660BE).

We acknowledge Diamond Light Source, Rutherford Appleton Laboratory, U.K., for the provision of synchrotron access to Beamline I15-1 (Proposal No. CY37860).

Appendix A. Supplementary data

Supplementary data to this article can be found online at https://doi.org/10.1016/j.carbpol.2025.123819.

References

Abbott, A. P. (2022). Deep eutectic solvents and their application in electrochemistry. *Current Opinion in Green and Sustainable Chemistry, 36*, Article 100649. https://doi.org/10.1016/j.cogsc.2022.100649

Abbott, A. P., Capper, G., Davies, D. L., Rasheed, R. K., & Tambyrajah, V. (2003). Novel solvent properties of choline chloride/urea mixtures. *Chemical Communications, 1*, 70–71. https://doi.org/10.1039/B210714G

Abranches, D. O., & Coutinho, J. A. P. (2023). Annual review of chemical and biomolecular engineering everything you wanted to know about deep eutectic solvents but were afraid to be told. *Annual Review of Chemical and Biomolecular Engineering 2023, 14*, 141–163. https://doi.org/10.1146/annurev-chembioeng

Athanasiadis, V., Grigorakis, S., Lalas, S., & Makris, D. P. (2018). Methyl β-cyclodextrin as a booster for the extraction for Olea europaea leaf polyphenols with a bio-based deep eutectic solvent. *Biomass Conversion and Biorefinery, 8*(2), 345–355. https://doi.org/10.1007/s13399-017-0283-5

Bhardwaj, V. K., & Purohit, R. (2023). A comparative study on inclusion complex formation between formononetin and β-cyclodextrin derivatives through multiscale classical and umbrella sampling simulations. *Carbohydrate Polymers, 310*, 120709. https://doi.org/10.1016/j.carbpol.2023.120729

Bracchini, G. A., Mangiacapre, E., lo Celso, F., Irving, D. J. M., Ottaviani, C., Righetti, G. I. C., … Triolo, A. (2024). Structural features of neat 5-hydroxymethylfurfural (HMF) in the liquid state. *Journal of Molecular Liquids, 410*, Article 125622. https://doi.org/10.1016/j.molliq.2024.125622

Brehm, M., & Kirchner, B. (2011). TRAVIS - A free analyzer and visualizer for Monte Carlo and molecular dynamics trajectories. *Journal of Chemical Information and Modeling, 51*(8), 2007–2023. https://doi.org/10.1021/ci200217w

Brehm, M., Thomas, M., Gehrke, S., & Kirchner, B. (2020). TRAVIS—A free analyzer for trajectories from molecular simulation. In *Journal of chemical physics 152(16), 164105*. Inc.: American Institute of Physics. https://doi.org/10.1063/5.0005078.

Brewster, M. E., & Loftsson, T. (2007). Cyclodextrins as pharmaceutical solubilizers. *Advanced Drug Delivery Reviews, 59*(7), 645–666. https://doi.org/10.1016/j.addr.2007.05.012

Bussi, G., Donadio, D., & Parrinello, M. (2007). Canonical sampling through velocity rescaling. *Journal of Chemical Physics, 126*(1). https://doi.org/10.1063/1.2408420

Cézard, C., Trivelli, X., Aubry, F., Djedaïni-Pilard, F., & Dupradeau, F.-Y. (2011). Molecular dynamics studies of native and substituted cyclodextrins in different media: 1. Charge derivation and force field performances. *Physical Chemistry Chemical Physics, 13*(33), 15103–15121. https://doi.org/10.1039/C1CP20854C

Chen, Y., Chen, W., Fu, L., Yang, Y., Wang, Y., Hu, X., … Mu, T. (2019). Surface tension of 50 deep eutectic solvents: Effect of hydrogen-bonding donors, hydrogen-bonding acceptors, other solvents, and temperature. *Industrial & Engineering Chemistry Research, 58*(28), 12741–12750. https://doi.org/10.1021/acs.iecr.9b00867

Ciobanu, A., Landy, D., & Fourmentin, S. (2013). Complexation efficiency of cyclodextrins for volatile flavor compounds. *Food Research International, 53*(1), 110–114. https://doi.org/10.1016/j.foodres.2013.03.048

Connors, K. A. (1997). The stability of Cyclodextrin complexes in solution. *Chemical Reviews, 97*(5), 1325–1358. https://doi.org/10.1021/cr960371r

Crini, G., Fourmentin, S., Fenyvesi, É., Torri, G., Fourmentin, M., & Morin-Crini, N. (2018a). Cyclodextrins, from molecules to applications. *Environmental Chemistry Letters, 16*(4), 1361–1375. https://doi.org/10.1007/s10311-018-0763-2

Crini, G., Fourmentin, S., Fenyvesi, É., Torri, G., Fourmentin, M., & Morin-Crini, N. (2018b). *Fundamentals and applications of cyclodextrins*. pp. 1–55. https://doi.org/10.1007/978-3-319-76159-6_1.

Darden, T., York, D., & Pedersen, L. (1993). Particle mesh Ewald: An N·log(N) method for Ewald sums in large systems. *The Journal of Chemical Physics, 98*(12), 10089–10092. https://doi.org/10.1063/1.464397

Decock, G., Landy, D., Surpateanu, G., & Fourmentin, S. (2008). Study of the retention of aroma components by cyclodextrins by static headspace gas chromatography. *Journal of Inclusion Phenomena and Macrocyclic Chemistry, 62*(3–4), 297–302. https://doi.org/10.1007/s10847-008-9471-z

Di Pietro, M. E., Colombo Dugoni, G., Ferro, M., Mannu, A., Castiglione, F., Costa Gomes, M., … Mele, A. (2019). Do Cyclodextrins encapsulate volatiles in deep eutectic systems? *ACS Sustainable Chemistry & Engineering, 7*(20), 17397–17405. https://doi.org/10.1021/acssuschemeng.9b04526

Dodda, L. S., De Vaca, I. C., Tirado-Rives, J., & Jorgensen, W. L. (2017). LigParGen web server: An automatic OPLS-AA parameter generator for organic ligands. *Nucleic Acids Research, 45*(W1), W331–W336. https://doi.org/10.1093/nar/gkx312

Dodda, L. S., Vilseck, J. Z., Tirado-Rives, J., & Jorgensen, W. L. (2017). 1.14*CM1A-LBCC: Localized bond-charge corrected CM1A charges for condensed-phase simulations. *Journal of Physical Chemistry B, 121*(15), 3864–3870. https://doi.org/10.1021/acs.jpcb.7b00272

Donze, C., & Coleman, A. W. (1993). B-CD inclusion complexes: Relative selectivity of terpene and aromatic guest molecules studied by competitive inclusion experiments. *Journal of Inclusion Phenomena and Molecular Recognition in Chemistry, 16*(1), 1–15. https://doi.org/10.1007/BF00708758

Dugoni, G. C., Di Pietro, M. E., Ferro, M., Castiglione, F., Ruellan, S., Moufawad, T., … Mele, A. (2019). Effect of water on deep eutectic solvent/β-Cyclodextrin systems. *ACS Sustainable Chemistry & Engineering, 7*(7), 7277–7285. https://doi.org/10.1021/acssuschemeng.9b00315

Dwamena, A. K. (2019). Recent advances in hydrophobic deep eutectic solvents for extraction. *Separations, 6*(1), Article 9. https://doi.org/10.3390/separations6010009

El Achkar, T., Moufawad, T., Ruellan, S., Landy, D., Greige-Gerges, H., & Fourmentin, S. (2020). Cyclodextrins: From solute to solvent. *Chemical Communications, 56*(23), 3385–3388. https://doi.org/10.1039/d0cc00460j

El Achkar, T., Moura, L., Moufawad, T., Ruellan, S., Panda, S., Longuemart, S., … Fourmentin, S. (2020). New generation of supramolecular mixtures: Characterization and solubilization studies. *International Journal of Pharmaceutics, 584*, Article 119443. https://doi.org/10.1016/j.ijpharm.2020.119443

El Masri, S., Ruellan, S., Zakhour, M., Auezova, L., & Fourmentin, S. (2022). Cyclodextrin-based low melting mixtures as a solubilizing vehicle: Application to non-steroidal anti-inflammatory drugs. *Journal of Molecular Liquids, 353*, Article 118827. https://doi.org/10.1016/j.molliq.2022.118827

Essmann, U., Perera, L., Berkowitz, M. L., Darden, T., Lee, H., & Pedersen, L. G. (1995). A smooth particle mesh Ewald method. *The Journal of Chemical Physics, 103*(19), 8577–8593. https://doi.org/10.1063/1.470117

Farooq, M. Q., Zeger, V. R., & Anderson, J. L. (2021). Comparing the extraction performance of cyclodextrin-containing supramolecular deep eutectic solvents versus conventional deep eutectic solvents by headspace single drop microextraction. *Journal of Chromatography A, 1658*, Article 462588. https://doi.org/10.1016/j.chroma.2021.462588

Ferreira, M., Jérôme, F., Bricout, H., Menuel, S., Landy, D., Fourmentin, S., Tilloy, S., & Monflier, E. (2015). Rhodium catalyzed hydroformylation of 1-decene in low melting mixtures based on various cyclodextrins and N,N′-dimethylurea. *Catalysis Communications, 63*, 62–65. https://doi.org/10.1016/j.catcom.2014.11.001

Gebhardt, J., Kleist, C., Jakobtorweihen, S., & Hansen, N. (2018). Validation and comparison of force fields for native Cyclodextrins in aqueous solution. *The Journal of Physical Chemistry B, 122*(5), 1608–1626. https://doi.org/10.1021/acs.jpcb.7b11808

Gonzalez Pereira, A., Carpena, M., García Oliveira, P., Mejuto, J. C., Prieto, M. A., & Simal Gandara, J. (2021). Main applications of cyclodextrins in the food industry as the compounds of choice to form host–guest complexes. *International Journal of Molecular Sciences, 22*(3), Article 1339. https://doi.org/10.3390/ijms22031339

Gui, C., Villarim, P., Lei, Z., & Fourmentin, S. (2024). VOC absorption in supramolecular deep eutectic solvents: Experiment and molecular dynamic studies. *Chemical Engineering Journal, 481*, Article 148708. https://doi.org/10.1016/j.cej.2024.148708

Gui, C., Xiang, D., Feng, M., Guo, C., & Fourmentin, S. (2025). Effective VOCs abatement using supramolecular deep eutectic solvents. *Separation and Purification Technology, 360*, Article 131121. https://doi.org/10.1016/j.seppur.2024.131121

Gutiérrez, A., Zamora, L., Benito, C., Atilhan, M., & Aparicio, S. (2022). Insights on novel type V deep eutectic solvents based on levulinic acid. *The Journal of Chemical Physics, 156*(9), Article 094504. https://doi.org/10.1063/5.0080470

Häusler, O., & Muller-Goymann, C. C. (1993). Properties and structure of aqueous solutions of Hydroxypropyl-beta-Cyclodextrin. *Starch Stärke, 45*, 183–187. https://doi.org/10.1002/star.19930450508

He, Y., Li, P., & Yalkowsky, S. H. (2003). Solubilization of fluasterone in cosolvent/cyclodextrin combinations. *International Journal of Pharmaceutics, 264*(1), 25–34. https://doi.org/10.1016/S0378-5173(03)00389-2

Hess, B., Kutzner, C., van der Spoel, D., & Lindahl, E. (2008). GROMACS 4: Algorithms for highly efficient, load-balanced, and scalable molecular simulation. *Journal of Chemical Theory and Computation, 4*(3), 435–447. https://doi.org/10.1021/ct700301q

Hollõczki, O., Macchiagodena, M., Weber, H., Thomas, M., Brehm, M., Stark, A., … Kirchner, B. (2015). Triphilic ionic-liquid mixtures: Fluorinated and non-fluorinated aprotic ionic-liquid mixtures. *ChemPhysChem, 16*(15), 3325–3333. https://doi.org/10.1002/cphc.201500473

Janicka, P., Kaykhaii, M., Płotka-Wasylka, J., & Gębicki, J. (2022). Supramolecular deep eutectic solvents and their applications. *Green Chemistry, 24*(13), 5035–5045. https://doi.org/10.1039/d2gc00906d

Jérôme, F., Ferreira, M., Bricout, H., Menuel, S., Monflier, E., & Tilloy, S. (2014). Low melting mixtures based on β-cyclodextrin derivatives and N,N′-dimethylurea as solvents for sustainable catalytic processes. *Green Chemistry, 16*(8), 3876–3880. https://doi.org/10.1039/C4GC00591K

Jorgensen, W. L., Maxwell, D. S., & Tirado-Rives, J. (1996). Development and testing of the OPLS all-atom force field on conformational energetics and properties of organic liquids. *Journal of the American Chemical Society, 118*, 11225–11236. https://doi.org/10.1021/ja9621760

Jorgensen, W. L., & Tirado-Rives, J. (2005). Potential energy functions for atomic-level simulations of water and organic and biomolecular systems. *Proceedings of the National Academy of Sciences of the United States of America, 102*, 6665–6670. https://doi.org/10.1073/pnas.0408037102

Kfoury, M., Auezova, L., Greige-Gerges, H., & Fourmentin, S. (2015). Promising applications of cyclodextrins in food: Improvement of essential oils retention, controlled release and antiradical activity. *Carbohydrate Polymers, 131*, 264–272. https://doi.org/10.1016/j.carbpol.2015.06.014

Kfoury, M., Auezova, L., Greige-Gerges, H., & Fourmentin, S. (2019). Encapsulation in cyclodextrins to widen the applications of essential oils. *Environmental Chemistry Letters, 17*(1), 129–143. https://doi.org/10.1007/s10311-018-0783-y

Kfoury, M., Auezova, L., Greige-Gerges, H., Ruellan, S., & Fourmentin, S. (2014). Cyclodextrin, an efficient tool for trans-anethole encapsulation: Chromatographic, spectroscopic, thermal and structural studies. *Food Chemistry, 164*, 454–461. https://doi.org/10.1016/j.foodchem.2014.05.052

Kfoury, M., Balan, R., Landy, D., Nistor, D., & Fourmentin, S. (2015). Investigation of the complexation of essential oil components with cyclodextrins. *Supramolecular Chemistry, 27*(9), 620–628. https://doi.org/10.1080/10610278.2015.1051977

Kfoury, M., Geagea, C., Ruellan, S., Greige-Gerges, H., & Fourmentin, S. (2019). Effect of cyclodextrin and cosolvent on the solubility and antioxidant activity of caffeic acid. *Food Chemistry, 278*, 163–169. https://doi.org/10.1016/j.foodchem.2018.11.055

Kfoury, M., Landy, D., Auezova, L., Greige-Gerges, H., & Fourmentin, S. (2014). Effect of cyclodextrin complexation on phenylpropanoids' solubility and antioxidant activity. *Beilstein Journal of Organic Chemistry, 10*, 2322–2331. https://doi.org/10.3762/bjoc.10.241

Kfoury, M., Landy, D., & Fourmentin, S. (2018). Characterization of cyclodextrin/volatile inclusion complexes: A review. *Molecules, 23*(5). https://doi.org/10.3390/molecules23051204

Kfoury, M., Landy, D., & Fourmentin, S. (2019). Contribution of headspace to the analysis of cyclodextrin inclusion complexes. *Journal of Inclusion Phenomena and Macrocyclic Chemistry, 93*(1–2), 19–32. https://doi.org/10.1007/s10847-018-0818-9

Kfoury, M., Landy, D., & Fourmentin, S. (2022). Combination of DES and macrocyclic host molecules: Review and perspectives. *Current Opinion in Green and Sustainable Chemistry, 36*, Article 100630. https://doi.org/10.1016/j.cogsc.2022.100630

Kfoury, M., Legrand, F.-X., Ruellan, S., & Fourmentin, S. (2024). Low melting mixtures: Neoteric green solvents for flavor formulation. *Journal of Molecular Liquids, 394*, Article 123696. https://doi.org/10.1016/j.molliq.2023.123696

Khuntawee, W., Karttunen, M., & Wong-Ekkabut, J. (2017). A molecular dynamics study of conformations of beta-cyclodextrin and its eight derivatives in four different solvents. *Physical Chemistry Chemical Physics, 19*(35), 24219–24229. https://doi.org/10.1039/c7cp04009a

Kida, T., Iwamoto, T., Fujino, Y., Tohnai, N., Miyata, M., & Akashi, M. (2011). Strong guest binding by Cyclodextrin hosts in competing nonpolar solvents and the unique crystalline structure. *Organic Letters, 13*(17), 4570–4573. https://doi.org/10.1021/ol2017627

Kivelä, H., Salomäki, M., Vainikka, P., Mäkilä, E., Poletti, F., Ruggeri, S., … Lukkari, J. (2022). Effect of water on a hydrophobic deep eutectic solvent. *Journal of Physical Chemistry B, 126*(2), 513–527. https://doi.org/10.1021/acs.jpcb.1c08170

Kolb, B., & LS, E. (2006). *Static headspace-gas chromatography: Theory and practice* (2nd ed.). Wiley.

Kumar, P., & Purohit, R. (2024). Driving forces and large scale affinity calculations for piperine/γ-cyclodxetrin complexes: Mechanistic insights from umbrella sampling simulation and DFT calculations. *Carbohydrate Polymers, 342*, Article 122350. https://doi.org/10.1016/j.carbpol.2024.122350

Kusmin, A., Lechner, R. E., Kammel, M., & Saenger, W. (2008). Native and methylated cyclodextrins with positive and negative solubility coefficients in water studied by SAXS and SANS. *Journal of Physical Chemistry B, 112*(41), 12888–12898. https://doi.org/10.1021/jp802031w

Landy, D., Fourmentin, S., Salome, M., & Surpateanu, G. (2000). Analytical improvement in measuring formation constants of inclusion complexes between β-Cyclodextrin and phenolic compounds. *Journal of Inclusion Phenomena and Macrocyclic Chemistry, 38*(1), 187–198. https://doi.org/10.1023/A:1008156110999

Li, G., Jiang, Y., Liu, X., & Deng, D. (2016). New levulinic acid-based deep eutectic solvents: Synthesis and physicochemical property determination. *Journal of Molecular Liquids, 222*, 201–207. https://doi.org/10.1016/j.molliq.2016.07.039

Li, P., Zhao, L., & Yalkowsky, S. H. (1999). Combined effect of cosolvent and cyclodextrin on solubilization of nonpolar drugs. *Journal of Pharmaceutical Sciences, 88*(11), 1107–1111. https://doi.org/10.1021/js990159d

Loftsson, T., & Brewster, M. E. (1996). Pharmaceutical applications of cyclodextrins. 1. Drug solubilization and stabilization. *Journal of Pharmaceutical Sciences, 85*(10), 1017–1025. https://doi.org/10.1021/js950534b

López-Salas, N., Vicent-Luna, J. M., Imberti, S., Posada, E., Roldán, M. J., Anta, J. A., … Del Monte, F. (2019). Looking at the "water-in-deep-eutectic-solvent" system: A dilution range for high performance eutectics. *ACS Sustainable Chemistry and Engineering, 7*(21), 17565–17573. https://doi.org/10.1021/acssuschemeng.9b05096

Marques, H. M. C. (2010). A review on cyclodextrin encapsulation of essential oils and volatiles. *Flavour and Fragrance Journal, 25*(5), 313–326. https://doi.org/10.1002/ffj.2019

Martinez, L., Andrade, R., Birgin, E. G., & Martínez, J. M. (2009). PACKMOL: A package for building initial configurations for molecular dynamics simulations. *Journal of Computational Chemistry, 30*(13), 2157–2164. https://doi.org/10.1002/jcc.21224

Martins, M. A. R., Pinho, S. P., & Coutinho, J. A. P. (2019). Insights into the nature of eutectic and deep eutectic mixtures. *Journal of Solution Chemistry, 48*(7), 962–982. https://doi.org/10.1007/s10953-018-0793-1

Maugeri, Z., & de María, P. (2012). Novel choline-chloride-based deep-eutectic-solvents with renewable hydrogen bond donors: Levulinic acid and sugar-based polyols. *RSC Advances, 2*(2), 421–425. https://doi.org/10.1039/C1RA00630D

Mohd Fuad, F., & Mohd Nadzir, M. (2022). The formulation and physicochemical properties of betaine-based natural deep eutectic solvent. *Journal of Molecular Liquids, 360*, Article 119392. https://doi.org/10.1016/j.molliq.2022.119392

Motoyama, K., Nagatomo, K., Abd Elazim, S. O., Hirayama, F., Uekama, K., & Arima, H. (2009). Potential use of 2-hydroxypropyl-beta-cyclodextrin for preparation of orally disintegrating tablets containing dl-alpha-tocopheryl acetate, an oily drug. *Chemical and Pharmaceutical Bulletin, 57*(11), 1206–1212. https://doi.org/10.1248/cpb.57.1206

Moufawad, T., Moura, L., Ferreira, M., Bricout, H., Tilloy, S., Monflier, E., … Fourmentin, S. (2019). First evidence of Cyclodextrin inclusion complexes in a deep eutectic solvent. *ACS Sustainable Chemistry and Engineering, 7*(6), 6345–6351. https://doi.org/10.1021/acssuschemeng.9b00044

Moura, L., Moufawad, T., Ferreira, M., Bricout, H., Tilloy, S., Monflier, E., … Fourmentin, S. (2017). Deep eutectic solvents as green absorbents of volatile organic pollutants. *Environmental Chemistry Letters, 15*(4), 747–753. https://doi.org/10.1007/s10311-017-0654-y

Nakhle, L., Kfoury, M., Fourmentin, S., Greige-Gerges, H., & Landy, D. (2024). Thermodynamic investigations on host/guest complexation in deep eutectic solvent/water mixtures. *Comptes Rendus Chimie, 27*, 1–9. https://doi.org/10.5802/crchim.304

Nakhle, L., Kfoury, M., Greige-Gerges, H., & Fourmentin, S. (2020). Effect of dimethylsulfoxide, ethanol, α- and β-cyclodextrins and their association on the solubility of natural bioactive compounds. *Journal of Molecular Liquids, 310*, Article 113156. https://doi.org/10.1016/j.molliq.2020.113156

Nakhle, L., Kfoury, M., Greige-Gerges, H., & Landy, D. (2023). Retention of a plethora of essential oils and aromas in deep eutectic solvent:Water:Cyclodextrin mixtures. *Journal of Inclusion Phenomena and Macrocyclic Chemistry, 103*(1–2), 35–44. https://doi.org/10.1007/s10847-022-01174-x

Parrinello, M., & Rahman, A. (1981). Polymorphic transitions in single crystals: A new molecular dynamics method. *Journal of Applied Physics, 52*(12), 7182–7190. https://doi.org/10.1063/1.328693

Rekharsky, M. V., & Inoue, Y. (1998). Complexation thermodynamics of Cyclodextrins. *Chemical Reviews, 98*(5), 1875–1918. https://doi.org/10.1021/cr970015o

Sánchez, P. B., González, B., Salgado, J., José Parajó, J., & Domínguez, Á. (2019). Physical properties of seven deep eutectic solvents based on l-proline or betaine. *The Journal of Chemical Thermodynamics, 131*, 517–523. https://doi.org/10.1016/j.jct.2018.12.017

Saokham, P., Muankaew, C., Jansook, P., & Loftsson, T. (2018). Solubility of cyclodextrins and drug/cyclodextrin complexes. *Molecules, 23*(5), 1161. https://doi.org/10.3390/molecules23051161

Savi, L. K., Carpiné, D., Waszczynskyj, N., Ribani, R. H., & Haminiuk, C. W. I. (2019). Influence of temperature, water content and type of organic acid on the formation, stability and properties of functional natural deep eutectic solvents. *Fluid Phase Equilibria, 488*, 40–47. https://doi.org/10.1016/j.fluid.2019.01.025

Shah, D., & Mjalli, F. S. (2014). Effect of water on the thermo-physical properties of reline: An experimental and molecular simulation based approach. *Physical Chemistry Chemical Physics, 16*(43), 23900–23907. https://doi.org/10.1039/c4cp02600d

Smith, E. L., Abbott, A. P., & Ryder, K. S. (2014). Deep eutectic solvents (DESs) and their applications. *Chemical Reviews, 114*(21), 11060–11082. https://doi.org/10.1021/cr300162p

Soper, A. K. (2011). *GudrunN and GudrunX: Programs for correcting raw neutron and X-ray diffraction data to differential scattering cross section. Ral technical reports: Ral-tr-2011-013, Rutherford Appleton Laboratory*.

Szejtli, J. (1998). Introduction and general overview of Cyclodextrin chemistry. *Chemical Reviews, 98*(5), 1743–1754. https://doi.org/10.1021/cr970022c

Triolo, A., Celso, F. L., Perez, J., & Russina, O. (2022). Solubility and solvation features of native cyclodextrins in 1-ethyl-3-methylimidazolium acetate. *Carbohydrate Polymers, 291*, Article 119622. https://doi.org/10.1016/j.carbpol.2022.119622

Triolo, A., Lo Celso, F., Fourmentin, S., & Russina, O. (2023). Liquid structure scenario of the archetypal supramolecular deep eutectic solvent: Heptakis(2,6-di- *O* -methyl)-β-cyclodextrin/levulinic acid. *ACS Sustainable Chemistry & Engineering*. https://doi.org/10.1021/acssuschemeng.3c01858

Triolo, A., Lo Celso, F., & Russina, O. (2020). Structural features of β-cyclodextrin solvation in the deep eutectic solvent, reline. *Journal of Physical Chemistry B, 124*(13), 2652–2660. https://doi.org/10.1021/acs.jpcb.0c00876

Ünlü, A. E., Arıkaya, A., & Takaç, S. (2019). Use of deep eutectic solvents as catalyst: A mini-review. *Green Processing and Synthesis, 8*(1), 355–372. https://doi.org/10.1515/gps-2019-0003

Usacheva, T., Pham, T. L., Nguyen, T. D., Kabirov, D., Alister, D., Vu, X. M., … Giancola, C. (2020). Host–guest inclusion complex of β-cyclodextrin and benzoic acid in water–ethanol solvents: Spectroscopic and thermodynamic characterization of complex formation. *Journal of Thermal Analysis and Calorimetry, 142*(5), 2015–2024. https://doi.org/10.1007/s10973-020-09807-4

Van Der Spoel, D., Lindahl, E., Hess, B., Groenhof, G., Mark, A. E., & Berendsen, H. J. C. (2005). GROMACS: Fast, flexible, and free. *Journal of Computational Chemistry, 26*(16), 1701–1718. https://doi.org/10.1002/jcc.20291

Vargaftik, N. B., Volkov, B. N., & Voljak, L. D. (1983). International tables of the surface tension of water. *Journal of Physical and Chemical Reference Data, 12*, 817–820. https://api.semanticscholar.org/CorpusID:97396344.

Villarim, P., Genty, E., Zemmouri, J., & Fourmentin, S. (2022). Deep eutectic solvents and conventional solvents as VOC absorbents for biogas upgrading: A comparative study. *Chemical Engineering Journal, 446*(Part1), Article 136875. https://doi.org/10.1016/j.cej.2022.136875

Villarim, P., Gui, C., Genty, E., Lei, Z., Zemmouri, J., & Fourmentin, S. (2024). Toluene absorption from laboratory to industrial scale: An experimental and theoretical study. *Separation and Purification Technology, 328*, Article 125070. https://doi.org/10.1016/j.seppur.2023.125070

Yu, G., Jie, K., & Huang, F. (2015). Supramolecular amphiphiles based on host–guest molecular recognition motifs. *Chemical Reviews, 115*(15), 7240–7303. https://doi.org/10.1021/cr5005315

Zhang, H., Ge, C., van der Spoel, D., Feng, W., & Tan, T. (2012). Insight into the structural deformations of Beta-Cyclodextrin caused by alcohol Cosolvents and guest molecules. *The Journal of Physical Chemistry B, 116*(12), 3880–3889. https://doi.org/10.1021/jp300674d